ACS SENSORS

Article

pubs.acs.org/acssensors

Rationally Modulate the Oxidase-like Activity of Nanoceria for Self-Regulated Bioassays

Hanjun Cheng,[†,‡] Shichao Lin,[†] Faheem Muhammad,[†] Ying-Wu Lin,[§] and Hui Wei*[,†,‡]

[†]Department of Biomedical Engineering, College of Engineering and Applied Sciences, Nanjing National Laboratory of Microstructures, Nanjing University, Nanjing, Jiangsu 210093, China

[‡]Collaborative Innovation Center of Chemistry for Life Sciences, State Key Laboratory of Analytical Chemistry for Life Science, Nanjing University, Nanjing, Jiangsu 210093, China

[§]School of Chemistry and Chemical Engineering, University of South China, Hengyang, Hunan 421001, China

Supporting Information

ABSTRACT: One of the current challenges in nanozyme-based technology is to rationally control the enzyme mimicking activities with suitable modulation strategies to mimic the complexity and functions of natural systems. In this regard, nanoceria has recently emerged as a promising nanozyme because of its unique enzyme mimicking properties. Herein, we demonstrated that the oxidase-like catalytic activity of nanoceria was rationally modulated in situ via proton-producing/consuming enzyme-catalyzed bioreactions, which formed the basis of self-regulated bioassays for determining the corresponding enzyme activity, as well as other important targets, such as nerve agents, drugs, and bioactive ions. More interestingly, the oxidase-like activity of nanoceria was cooperatively modulated with the aid of adenosine triphosphate, thus improving the analytical performance of such self-regulated bioassays. The current study not only demonstrated regulatory strategies to modulate the nanozymes' activities, but also established a facile approach to designing self-regulated bioassays.

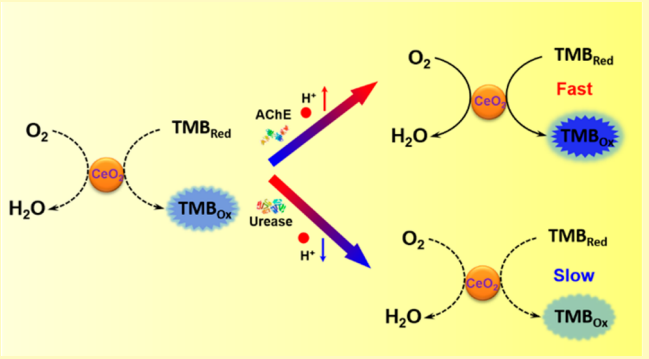

KEYWORDS: *nanozymes, nanoceria, self-regulated bioassays, oxidase mimics, functional nanomaterials, artificial enzymes, acetylcholinesterase, urease*

Natural enzymes play central roles in all biological processes.[1,2] They have also been widely exploited for various practical applications such as in biomedical analysis, food industry, and environmental protection.[3] However, their great potential has not yet been fully achieved owing to their intrinsic drawbacks, such as ease-of-denaturation and high cost. Therefore, intensive efforts have been devoted to mimicking natural enzymes with various materials.[4] Among them, a number of catalytic nanomaterials have recently been explored to imitate natural enzymes.[5−9] These nanomaterial-based mimics (i.e., nanozymes) have attracted considerable attentions due to their unique advantages over natural enzymes and even conventional enzyme mimics.[5−34] For example, oxidase has been successfully imitated using gold nanoparticles, nanoceria, and so forth.[35−37] Despite considerable progress made in the field of nanozymes, most of the currently developed nanozymes still face several challenges such as limited specificities and catalytic activities when compared with their natural counterparts.[6,7] To circumvent these challenges, tremendous efforts have recently been made such as in functionalizing the exterior surface of nanozymes with suitable functional groups and designing novel nanozymes with structures similar to the active site of natural enzymes.[18,38,39]

On the other hand, the catalytic activities of natural enzymes are sophisticatedly modulated via numerous regulatory mechanisms in biological systems. For instance, previous investigation provided evidence in support of a proton-dependent regulatory mechanism for mitochondrial nicotinamide-nucleotide transhydrogenase.[40] Moreover, the activities of natural enzymes are modulated at multiple levels. For example, the proteolytic activity of $HtrA_2$ (high-temperature requirement protease A_2) was additively enhanced by sequentially modulating the N-terminal and C-terminal with corresponding ligands.[41] With this deep understanding in modulating natural enzymes' activities, a few promising strategies to efficiently tune the catalytic activity of nanozymes have been recently demonstrated.[38,39,42−44] Despite of these developments, the strategies for modulating the activities of nanozymes, especially in an in situ manner, are still quite limited. Moreover, the multilevel modulation of nanozymes has also remained largely unexplored. Encouraged by the previous success of natural

Received: August 13, 2016
Accepted: October 25, 2016
Published: October 25, 2016

DOI: 10.1021/acssensors.6b00500
ACS Sens. 2016, 1, 1336−1343

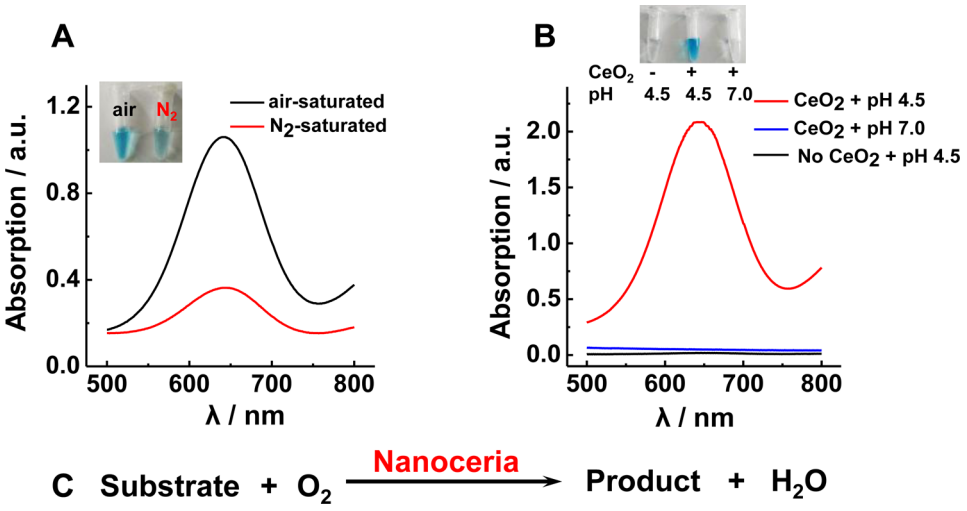

Figure 1. Oxidase-like activity of nanoceria. (A) O_2-dependent catalytic oxidation of 500 μM TMB with 100 μg/mL nanoceria in 100 mM PBS (pH 4.5). (B) pH-dependent catalytic oxidation of 500 μM TMB with O_2 in the absence and presence of 100 μg/mL nanoceria. Insets: the corresponding photo of the reaction solutions. (C) Oxidation of a substrate with O_2 catalyzed by oxidase-like nanoceria, producing oxidized product and water.

enzymes and nanozymes modulation, here we developed versatile self-regulated bioassays by in situ modulating the oxidase-like activity of nanoceria through proton-producing (or proton-consuming) enzymatic reactions. We further demonstrated that the bioassays could be cooperatively modulated when bioactive molecules (e.g., adenosine triphosphate (ATP)) were introduced as a secondary modulator. With the currently developed bioassays, several biomedically important enzymes (such as acetylcholinesterase (AChE), esterase, and urease), bioactive small molecules (such as organophosphorus based nerve agents and drugs) and ions (such as F^-) have been facilely detected.

RESULTS AND DISCUSSION

Nanoceria with Oxidase-like Activity. The nanoceria was prepared with the method previously developed by one of us.[45] The formation of nanoceria was confirmed by transmission electron microscopy (TEM) imaging, showing an average size of 3.8 nm (Figure S1). It was consistent with dynamic light scattering (DLS) measurement (Figure S2). The nanoceria was further characterized by X-ray diffraction (XRD) and X-ray photoelectron spectroscopy (XPS), showing highly crystalline features and mixed valence states of Ce^{3+} and Ce^{4+} (Figures S3 and S4A), which would play key roles in its enzyme mimicking properties.

The oxidase-like activity of nanoceria was then investigated. Numerous studies have demonstrated that nanoceria exhibited multienzyme mimicking activities (such as superoxide dismutase and catalase mimicking activities), which were originated from its mixed valence states of Ce^{3+} and Ce^{4+}, as well as the presence of oxygen vacancies.[43,46−50] Recently, it was suggested that nanoceria also exhibited oxidase-like catalytic activities.[36] However, there are still concerns in whether nanoceria acts as an oxidase mimic or just as an oxidant.[51] In this regard, it is essential to investigate the catalytic behavior and mechanism of oxidase-like property of nanoceria.

First, the O_2-dependent catalytic activity of nanoceria was investigated to confirm its oxidase-like property. As shown in Figure 1A, TMB (3,3′,5,5′-tetramethylbenzidine), a typical oxidase chromogenic substrate, was oxidized to its colored product (i.e., oxidized TMB, TMB_{ox}) in the air-saturated reaction solution containing nanoceria. The characteristic absorption peak of TMB_{ox} centered at 652 nm was also monitored by absorption spectroscopy. In contrast, the TMB oxidation was significantly inhibited in the N_2-saturated reaction solution. These results indicated that O_2 was necessary for the catalytic reaction, validating the oxidase-like activity of nanoceria.

Previous studies have showed that the catalytic activity of nanoceria was pH-dependent and the optimal activity was usually observed at acidic conditions.[36,52] Therefore, the oxidation of TMB with oxidase-like nanoceria was also evaluated at different pH values. As shown in Figure 1B, when the catalysis was carried out in neutral solution (i.e., 100 mM PBS, pH 7.0) containing nanoceria, the reaction solution remained colorless and the corresponding absorption spectrum did not show any obvious peak at 652 nm. This indicated that no TMB_{ox} was produced, which in turn demonstrated that the catalytic reaction did not proceed due to the extremely low activity of nanoceria at neutral pH. On the other hand, TMB was efficiently oxidized to colored TMB_{ox} when the catalytic reaction was performed in acidic solution (i.e., 100 mM PBS, pH 4.5) containing nanoceria. Further detailed pH-dependent study revealed that the oxidase-like activity of nanoceria quickly increased along with the decrease of pH value of reaction solutions and reached its plateau at ca. pH 4.5 (Figure S6). Therefore, taking account of these similarities between oxidases and nanoceria, we proposed that the nanoceria indeed acted as an oxidase mimic rather than an oxidant under the currently studied conditions (Figure 1C).

Reaction Mechanism for Oxidase-like Activity of Nanoceria. The possible mechanism for the oxidase-like activity of nanoceria was then elucidated. The steady-state kinetics studies under acidic conditions (i.e., 100 mM PBS, pH 4.5) showed that the nanoceria-catalyzed TMB oxidation reaction obeyed the Michaelis−Menten kinetics (Figure S7 and Table S2). The obtained Michaelis−Menten constant (K_m) of the nanoceria for TMB was ca. 0.42 mM, which was comparable to or even smaller than that for other nanoceria-based oxidase mimics, suggesting that our nanoceria possessed a higher affinity toward TMB.[36]

DOI: 10.1021/acssensors.6b00500
ACS Sens. 2016, 1, 1336−1343

To further elucidate the molecular mechanism for the oxidase mimicking activity of nanoceria, the possible reaction intermediates (such as H_2O_2, $OH^•$, and $O_2^{•-}$) that always involved in oxidase-catalyzed reactions were then identified. First, whether H_2O_2 was one of the intermediates was investigated, as H_2O_2 is the reduction product of O_2 for a large number of natural oxidases (such as glucose oxidase) and their mimics (such as Au nanoparticles).[35] Furthermore, if H_2O_2 were produced, it would further trigger the peroxidase mimicking property of nanoceria. This would in turn catalyze the oxidation of TMB with the intermediate H_2O_2, presenting nanoceria with an apparent oxidase-like activity. With such hypothesis, the adding of catalase, an enzyme that efficiently catalyzes the disproportionation of H_2O_2 into O_2 and H_2O, would substantially eliminate the produced intermediate H_2O_2 and thus inhibit the catalytic oxidation of TMB. As shown in Figure S8, the adding of catalase into the catalytic reaction solution containing nanoceria and TMB at pH 4.5 still led to a blue-colored solution. More interestingly, the kinetics of the produced TMB_{ox} was not significantly different from that obtained by using the same amount of bovine serum albumin (BSA) as a control. Both of these experiments suggested that H_2O_2 may not play a critical role in the catalytic reactions at pH 4.5. Then, the possibility of in situ forming $OH^•$ at the surface of nanoceria was studied. Terephthalic acid, a specific fluorescence probe for $OH^•$, was chosen to detect $OH^•$. No fluorescence emission peaks were observed after the addition of nanoceria, suggesting that no $OH^•$ was produced (data not shown). Interestingly, when hydroethidine, an $O_2^{•-}$ specific fluorescence probe, was added into the nanoceria solution at pH 4.5, a pronounced fluorescent emission at 610 nm appeared (Figure S9), demonstrating the formation of $O_2^{•-}$ at the surface of nanoceria. However, when hydroethidine was added into nanoceria solution at pH 7.0, only extremely weak fluorescent emission peak was observed, suggesting that very limited $O_2^{•-}$ was produced under the neutral condition. Previous studies have suggested that defect sites on nanoceria played critical roles in its enzyme-mimicking property.[49,52,53] On the other hand, several studies also reported that the defects on the surface of nanomaterials were active sites for catalysis.[54,55] In this regard, it was reasonable to suppose that the absorbed O_2 at the defect sites of nanoceria could be reduced to $O_2^{•-}$ by Ce^{3+} (Figure 2). Taking together the above-discussed results, it suggested that $O_2^{•-}$ was the main intermediate involved in the oxidase mimicking activity of nanoceria.

$$O_2 + Ce^{3+}(CeO_2) \longrightarrow O_2^{•-} + Ce^{4+}(CeO_2) \quad (1)$$

$$O_2^{•-} + TMB_{red} \longrightarrow H_2O + TMB_{ox} \quad (2)$$

$$CeO_2 + TMB_{red} \longrightarrow Ce_2O_3 + TMB_{ox} \quad (3)$$

$$Ce_2O_3 + O_2^{•-} + 2H^+ \longrightarrow CeO_2 + H_2O \quad (4)$$

Figure 2. Proposed mechanism for the oxidase-like activity of nanoceria.

Furthermore, the surface states of nanoceria before and after catalytic oxidation of TMB were monitored by using XPS. As shown in Figure S4, the XPS spectra of Ce(3d) peaks of nanoceria remained almost unchanged before and after the catalysis. Moreover, the quantitative analysis revealed the slight variation of Ce^{3+} content before and after the catalysis (Table S1), which essentially suggested that Ce^{3+}/Ce^{4+} at the surface of nanoceria had been recycled. This substantially demonstrated that nanoceria served as an oxidase-like catalyst toward TMB oxidation. Based on these results, a possible mechanism for the oxidase-like activity of nanoceria was proposed (Figure 2). Briefly, under acidic solutions, O_2 would be first adsorbed onto the surface of nanoceria, where it was converted into $O_2^{•-}$. Meanwhile, the surface Ce^{4+} of nanoceria was reduced to Ce^{3+} with concomitant oxidation of TMB to TMB_{ox}. The reduced Ce^{3+} was subsequently reoxidized to Ce^{4+} by the in situ produced $O_2^{•-}$. Alternatively, TMB could also be directly oxidized to TMB_{ox} with $O_2^{•-}$.

In Situ Modulating Oxidase-like Activity of Nanoceria. After understanding of the oxidase-like activity of the nanoceria, the in situ modulation of its catalytic activity was explored. As demonstrated above, the oxidase-like activity of nanoceria was pH-dependent. Therefore, a proton-dependent regulatory mechanism for in situ modulating its activity was proposed by introducing proton-producing (or proton-consuming) enzymes.

To demonstrate the hypothesis, AChE, a proton-producing enzyme, and its substrate acetylcholine (ACh) were employed as a proof-of-concept to in situ modulate the catalytic activity of nanoceria (Figure 3). AChE catalyzes the hydrolysis of ACh to produce choline and acetic acid (i.e., the source of proton). As shown in Figure 3A, when the catalysis was carried out in 5 mM PBS (pH 7.0) containing nanoceria, TMB, and ACh but no AChE, very limited amount of TMB_{ox} was formed as indicated by the almost colorless solution and very weak absorption peak at 652 nm. In sharp contrast, when AChE was added into the reaction solution, prominently colored TMB_{ox} along with the strong absorption peak at 652 nm was observed. These results demonstrated that the in situ produced protons by the AChE catalyzed reaction acted as a modulator to activate the oxidase-like activity of nanoceria, which in turn enhanced the catalytic oxidation of TMB. To further confirm that the enhanced catalytic activity of nanoceria was originated from the in situ produced protons, the pH values of the reaction solutions were continuously monitored. As shown in Figure 3B, the pH of the reaction solution with AChE gradually decreased from 6.7 to 4.3 within around 10 min, while the pH of the reaction solution without AChE remained almost unchanged during the measurement. These results thus demonstrated that the nanoceria's catalytic activity could be effectively modulated by in situ forming protons with proton-producing enzymes (such as AChE).

Self-Regulated Bioassays with Oxidase-like Nanoceria. By exploring the in situ regulatory mechanism, we envisioned that versatile self-regulated bioassays could be developed by modulating the oxidase-like activity of nanoceria with proton-producing (or proton-consuming) enzymes. The demonstration of such bioassays was first exemplified by facile colorimetric detection of AChE using nanoceria. AChE plays a key role in the central and peripheral nervous systems, as the substantial accumulation of its natural substrate ACh might result in organ failure and even death.[56] Furthermore, the overhydrolysis of ACh by AChE can also lead to Alzheimer's disease by accelerating the aggregation of amyloid β-peptides into amyloid plaques.[57,58] Therefore, detection of AChE is of great importance for bioanalytical and biomedical applications.[58,59]

As shown in Figure S10, in the absence of AChE, since no acetic acid was produced, the detection solution of 5 mM PBS

DOI: 10.1021/acssensors.6b00500
ACS Sens. 2016, 1, 1336−1343

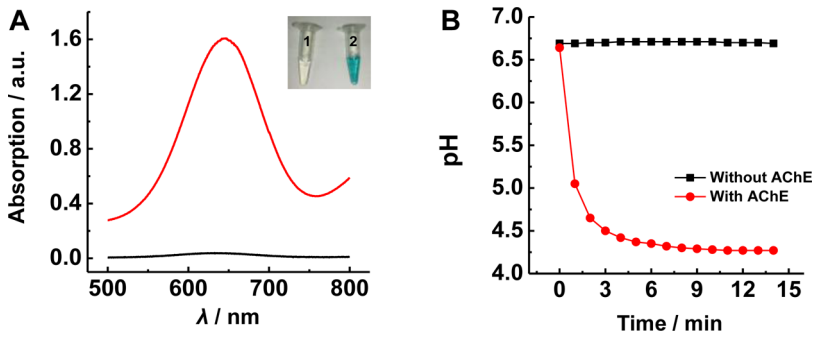

Figure 3. In situ modulation of oxidase-like activity of nanoceria with proton-producing enzyme (i.e., AChE). (A) Absorption spectra of the reaction solution (5 mM PBS, pH 7.0) containing 100 μg/mL nanoceria, 500 μM TMB, and 50 mM ACh, with AChE (red curve, vial 2) and without 1.4 U AChE (black curve, vial 1). Inset: the corresponding photo. (B) Time-dependent pH changes of the reaction solution (5 mM PBS, pH 7.0) containing 100 μg/mL nanoceria, 500 μM TMB, and 50 mM ACh, with AChE (red curve) and without 1.4 U AChE (black curve).

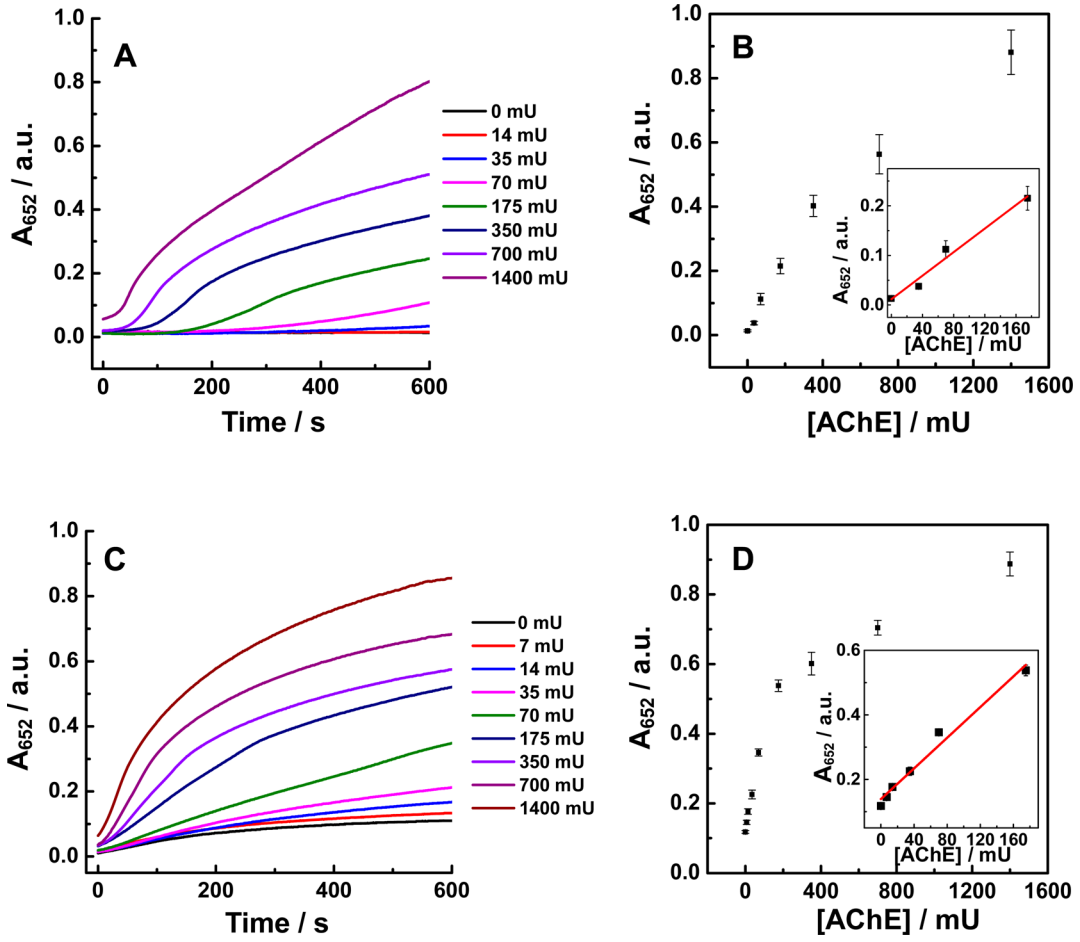

Figure 4. Kinetic plots of A_{652} for different concentrations of AChE in 5 mM PBS (pH 7.0) containing 100 μg/mL nanoceria, 500 μM TMB and 50 mM ACh in the absence (A) and presence (C) of 1 mM ATP. Dependence of A_{652} on AChE concentrations in the absence (B) and presence (D) of 1 mM ATP. Insets: linear range of A_{652} versus concentrations of AChE. Error bars indicate standard deviations of three independent measurements.

at pH 7.0 remained neutral and nearly no TMB_{ox} was formed. In the presence of AChE, however, the produced acetic acid lowered the pH of the detection solution, thus positively regulating the nanoceria catalyzed oxidation of TMB to TMB_{ox}. The bioassay of AChE was performed by monitoring the time-dependent absorption at 652 nm (i.e., A_{652}). As shown in Figure 4, by using A_{652} at 600 s as the signal readout, the recorded A_{652} increased with the increase of AChE activity and exhibited a linear response toward AChE activity ranging from 35 mU to 175 mU (A_{652} = 0.0012 × [AChE] mU^{-1} + 0.0012). The detection limit was determined to be around 25 mU ($S = 3\sigma$).

To improve the analytical performance of the proposed assay for AChE, the activity of nanoceria should be further enhanced. Previous study suggested that bioactive molecules like ATP could modulate the activities of nanozymes.[44,60,61] For instance, it was reported that the oxidase mimetic activity of nanoceria could be enhanced by the energy released from ATP hydrolysis.[44] Encouraged by these interesting phenomena, here ATP was introduced as a secondary modulator to

DOI: 10.1021/acssensors.6b00500
ACS Sens. 2016, 1, 1336−1343

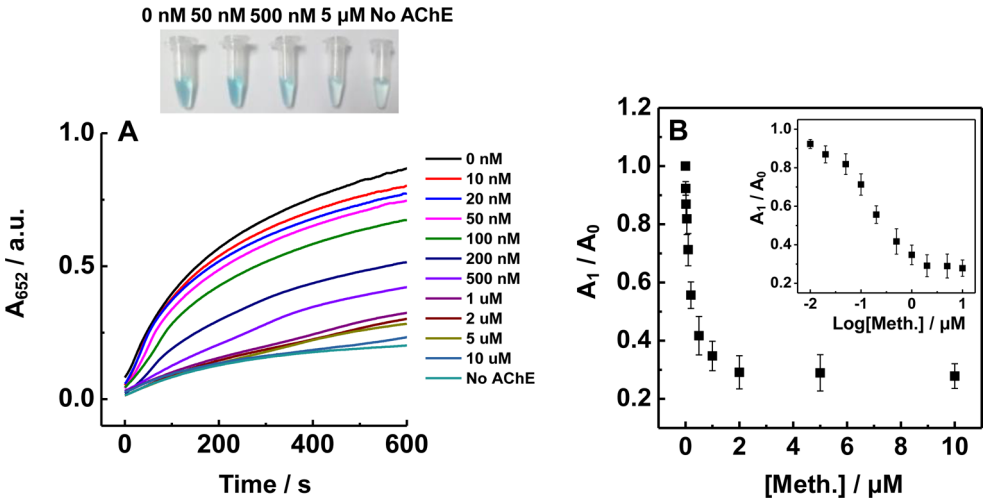

Figure 5. (A) Kinetic plots of A_{652} values for the reaction mixtures containing 100 μg/mL nanoceria, 500 μM TMB, 50 mM ACh, 1 mM ATP, 1.4 U AChE and different concentrations of methyl-paraoxon. Inset: the corresponding photo. (B) Plots of A_1/A_0 versus methyl-paraoxon concentration. Inset: plots of A_1/A_0 versus the logarithm of the methyl-paraoxon concentration. A_0, the A_{652} value in the absence of methyl-paraoxon; A_1, the A_{652} value in the presence of methyl-paraoxon; Meth., abbreviation for methyl-paraoxon. Error bars indicate standard deviations of three independent measurements.

cooperatively modulate the oxidase-like activity of nanoceria for enhanced bioassay toward AChE. The introduction of ATP indeed effectively enhanced the analytical performance of the self-regulated colorimetric assay. As shown in Figure 4C, as low as 7 mU AChE resulted in a distinguished difference of A_{652} from that without AChE. As a comparison, 14 mU AChE exhibited almost identical A_{652} as that without AChE when ATP was absent (Figure 4A). Moreover, a linear response from 7 to 175 mU for AChE activity to A_{652} (A_{652} = 0.0024 × [AChE] mU^{-1} + 0.137) and an improved detection limit of 3.5 mU ($S = 3\sigma$) were obtained (Figure 4D). The performance of the current bioassay was compared with conventional method, showing several advantages (such as high temporal solution, small sample volume and enzymatic turnovers) (Figure S11 and Table S3). The selectivity of the current bioassay was also evaluated, showing excellent specificity toward AChE detection (Figure S12). Careful analysis of Figure 4A and C revealed that ATP initially promoted the catalytic reaction but potentially inhibited the catalytic reaction in prolonged reactions. Such a phenomenon could not be well explained by the previously proposed mechanism,[44] suggesting that ATP played quite complicated roles in modulating the nanoceria's oxidase mimicking activities. For instance, the presence of ATP may eventually interact with the nanoceria by forming potential Ce−PO_4 complexes and thus inhibit its catalytic activity through shielding its active centers. The exact mechanism for the effects of ATP on the catalytic reactions is currently under investigation and will be reported in due course.

It should be pointed out that our self-regulated bioassay strategy is versatile and could be extended to other proton-producing enzymes (such as esterase, glutathione transferase, etc.). To demonstrate such versatility, the colorimetric detection of esterase was successfully carried out (Figure S13).

Moreover, the biomedical applications of the self-regulated bioassay strategy were further validated by determination of organophosphorus-based nerve agents. These organophosphate neurotoxins, as extensively used in modern agriculture, pose a great danger to our environment and health.[62] They can irreversibly inhibit the activity of AChE and cause acute toxicity.[62] Based on such inhibitory effects, a facile colorimetric method for monitoring these neurotoxins was established here (Figure S14). For this purpose, methyl-paraoxon, one of the most commonly used nerve agents, was chosen as a model to demonstrate the feasibility for nerve agent assay. As shown in Figure 5, after incubation of AChE with methyl-paraoxon, a distinct color gradient was observed for the different concentrations of methyl-paraoxon. This could be ascribed to the gradual inhibition of AChE activity with the increase amount of methyl-paraoxon, which in turn led to a deaccelerated activation of nanoceria activity toward TMB oxidation. When the assay was quantitatively followed by absorption spectroscopy (Figure 5B), as low as 10 nM methyl-paraoxon led to observable an inhibition of A_{652}. As shown in Figure 5B, by plotting the absorption ratios of A_{652} (A_1/A_0, A_0 and A_1 represent the A_{652} values in the absence and presence of methyl-paraoxon, respectively) versus the logarithm of the methyl-paraoxon concentrations, a sigmoidal profile was obtained. The IC_{50} (half-maximal inhibitory concentration) was calculated to be ca. 300 nM, which was consistent with previous reports.[59] It should be noted that the current bioassay is also applicable to screening other inhibitory reagents (such as potential drugs) toward AChE (Figure S15).

In nature, both positive and negative regulatory mechanisms are involved in finely modulating enzymes activities. Inspired by this, after achieving the positive modulation of the oxidase-like activity of nanoceria with proton-producing enzymes, we reasoned that the catalytic activity of nanoceria should be suppressed with proton-consuming enzymes. For this purpose, urease, a proton-consuming enzyme, was employed as an example to demonstrate our hypothesis. As shown in Figure S16, when the catalytic reaction was performed in the absence of urease, prominently colored TMB_{ox} was formed, indicating the catalytic oxidation of TMB. On the contrary, in the presence of urease, the reaction solution remained colorless and no absorption peak at 652 nm was observed. These results demonstrated that the catalytic activity of nanoceria was substantially suppressed by urease-catalyzed hydrolysis of urea and subsequent pH increase of the reaction solution (Figure S17).

DOI: 10.1021/acssensors.6b00500
ACS Sens. 2016, 1, 1336−1343

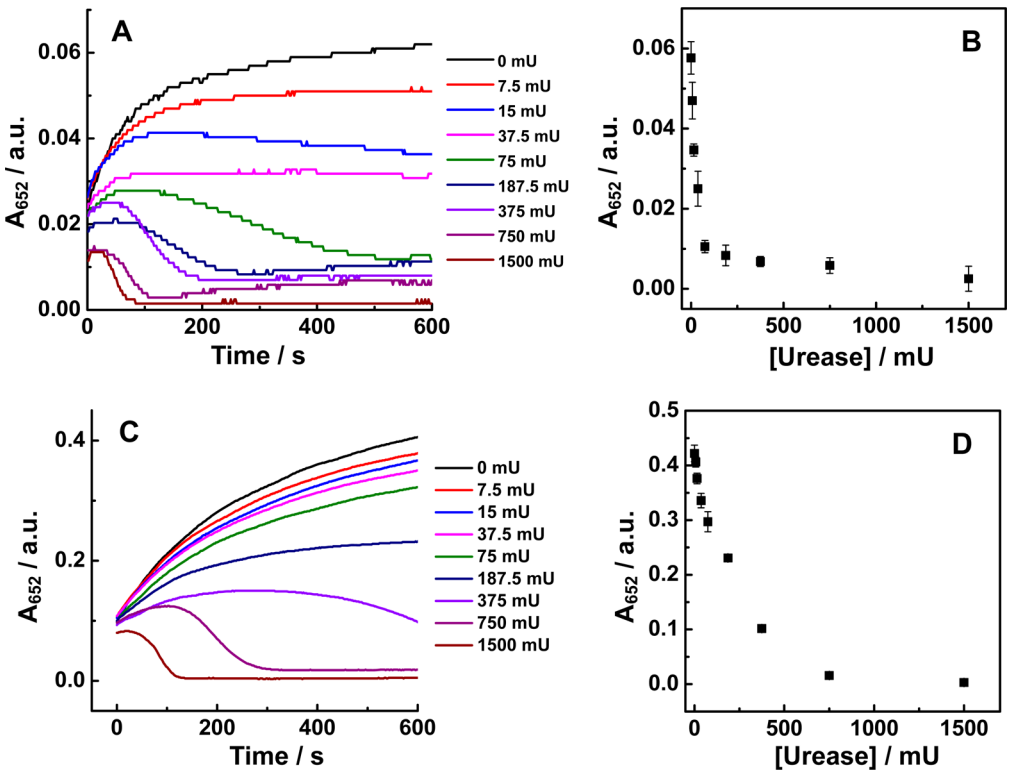

Figure 6. Kinetic plots of A_{652} for different concentrations of urease in 5 mM PBS (pH 4.5) containing 40 μg/mL nanoceria, 500 μM TMB and 50 mM urease in the absence (A) and presence (C) of 1 mM ATP. Dependence of A_{652} on urease concentrations in the absence (B) and presence (D) of 1 mM ATP. Error bars indicate standard deviations of three independent measurements.

Based on this negative regulatory mechanism, a colorimetric approach for determining urease activity was developed (Figure S18). The bioassay of urease was performed by monitoring the time-dependent absorption at 652 nm (i.e., A_{652}). As shown in Figure 6A and B, A_{652} decreased with the increase of urease activity from 0 to 75 mU. Then a plateau was reached. Interestingly, the introduction of ATP as the secondary modulator into the bioassay not only led to remarkably enhanced A_{652} values but also significantly broadened the dynamic range of urease activity (i.e., from 0−75 to 0−750 mU) (Figures 6C and D, and S20−S22). Compared to the AChE bioassay in the absence and presence of ATP, the significant difference for urease bioassay in the absence and presence of ATP might be attributed to the ATP-induced pH changes (Figure S19). As a further demonstration of the versatility of the above negatively modulated bioassay, we applied the assay for evaluating the potency of the proton-consuming enzymes' inhibitors. In this regard, fluoride ion (F^-), an inhibitor of urease, was investigated in our proof-of-concept experiments (Figure S23). As shown in Figure S24, with the increase of F^- concentration from 0 to 5 mM, a clear color gradient from colorless to blue was observed, accompanied by the increase of A_{652}. As shown in Figure S24B, by plotting the absorption ratios of A_{652} (A_1/A_0, A_0 and A_1 represent the A_{652} values in the absence and presence of urease, respectively) versus the logarithm of the F^- concentrations, a sigmoidal profile was obtained. The IC_{50} for 1.5 U urease was calculated to be around 750 μM.

CONCLUSIONS

In summary, in situ modulation of the oxidase-like catalytic activity of nanoceria was achieved with both proton-producing and proton-consuming enzymes. Highly sensitive self-regulated bioassays have been subsequently developed for detection of biomedically important enzymes and other bioactive targets (such as nerve agents, drugs, ions) via cooperatively modulating the activity of nanoceria. The current bioassays exhibited unique advantages (such as wider dynamic range) with respect to previously reported methods (Table S4). Though in the current study, only the colorimetric substrates were used for the bioassays, other substrates (such as fluorescent ones and Raman-active ones) could also be employed in the future study for even better performance. Moreover, other nanozymes with pH-dependent activities could be explored for developing such bioassays. When the proton-producing (or proton-consuming) enzymes are further conjugated with other biorecognition elements (such as antibodies, aptamers, DNAzymes, etc.), more targets of interest would be detected based on the currently developed strategies. These investigations are currently underway and will be reported in due course. In short, the current study not only provides a new strategy to rationally modulate the nanozymes activity,[63,64] but also opens an innovative approach to constructing facile bioassays.

ASSOCIATED CONTENT

Supporting Information

The Supporting Information is available free of charge on the ACS Publications website at DOI: 10.1021/acssensors.6b00500.

Additional figures with associated discussion (PDF)

DOI: 10.1021/acssensors.6b00500
ACS Sens. 2016, 1, 1336−1343

AUTHOR INFORMATION

Corresponding Author

*E-mail: weihui@nju.edu.cn. Tel: +86-25-83593272. Fax: +86-25-83594648. Web: http://weilab.nju.edu.cn/.

Author Contributions

The manuscript was written through contributions of all authors. All authors have given approval to the final version of the manuscript.

Notes

The authors declare the following competing financial interest(s): H.W. and H.C. are co-authors on patent applications.

ACKNOWLEDGMENTS

This work was supported by National Natural Science Foundation of China (21405079, 21405081, 21550110189), Natural Science Foundation of Jiangsu Province (BK20130561), 973 Program (2015CB659400), PAPD program, Fundamental Research Funds for Central Universities (no. 20620140617, 20620140627), Shuangchuang Program of Jiangsu Province, Six Talents Summit Program of Jiangsu Province, Open Funds of the State Key Laboratory of Electroanalytical Chemistry (SKLEAC201501), Open Funds of the State Key Laboratory of Analytical Chemistry for Life Science (SKLACLS1404), China Postdoctoral Science Foundation (153331), and Thousand Talents Program for Young Researchers. We thank Professor Lanqun Mao at Institute of Chemistry, Chinese Academy of Sciences for insightful discussions.

REFERENCES

(1) Gray, H. B.; Winkler, J. R. Electron transfer in proteins. *Annu. Rev. Biochem.* **1996**, *65*, 537−561.

(2) Erler, J. T.; Bennewith, K. L.; Nicolau, M.; Dornhofer, N.; Kong, C.; Le, Q. T.; Chi, J. T. A.; Jeffrey, S. S.; Giaccia, A. J. Lysyl oxidase is essential for hypoxia-induced metastasis. *Nature* **2006**, *440*, 1222−1226.

(3) Heller, A.; Feldman, B. Electrochemical glucose sensors and their applications in diabetes management. *Chem. Rev.* **2008**, *108*, 2482−2505.

(4) Breslow, R. *Artificial enzymes*, 1st ed.; Wiley: Weinheim, 2005.

(5) Pasquato, L.; Pengo, P.; Scrimin, P. Nanozymes: Functional nanoparticle-based catalysts. *Supramol. Chem.* **2005**, *17*, 163−171.

(6) Wei, H.; Wang, E. K. Nanomaterials with enzyme-like characteristics (nanozymes): next-generation artificial enzymes. *Chem. Soc. Rev.* **2013**, *42*, 6060−6093.

(7) Wang, X. Y.; Hu, Y. H.; Wei, H. Nanozymes in bionanotechnology: from sensing to therapeutics and beyond. *Inorg. Chem. Front.* **2016**, *3*, 41−60.

(8) Gao, L. Z.; Yan, X. Y. Nanozymes: an emerging field bridging nanotechnology and biology. *Sci. China: Life Sci.* **2016**, *59*, 400−402.

(9) Wang, X. Y.; Guo, W. J.; Hu, Y. H.; Wu, J. J. X.; Wei, H. *Nanozymes: next wave of artificial enzymes*; Springer: Heidelberg, 2016.

(10) Manea, F.; Houillon, F. B.; Pasquato, L.; Scrimin, P. Nanozymes: Gold-nanoparticle-based transphosphorylation catalysts. *Angew. Chem., Int. Ed.* **2004**, *43*, 6165−6169.

(11) Gao, L. Z.; Zhuang, J.; Nie, L.; Zhang, J. B.; Zhang, Y.; Gu, N.; Wang, T. H.; Feng, J.; Yang, D. L.; Perrett, S.; Yan, X. Intrinsic peroxidase-like activity of ferromagnetic nanoparticles. *Nat. Nanotechnol.* **2007**, *2*, 577−583.

(12) Fan, K.; Cao, C.; Pan, Y.; Lu, D.; Yang, D.; Feng, J.; Song, L.; Liang, M.; Yan, X. Magnetoferritin nanoparticles for targeting and visualizing tumour tissues. *Nat. Nanotechnol.* **2012**, *7*, 459−464.

(13) Wang, Q.; Zhang, L.; Shang, C.; Zhang, Z.; Dong, S. Triple-enzyme mimetic activity of nickel-palladium hollow nanoparticles and their application in colorimetric biosensing of glucose. *Chem. Commun.* **2016**, *52*, 5410−5413.

(14) Guo, Y.; Deng, L.; Li, J.; Guo, S.; Wang, E.; Dong, S. Hemin-Graphene Hybrid Nanosheets with Intrinsic Peroxidase-like Activity for Label-free Colorimetric Detection of Single-Nucleotide Polymorphism. *ACS Nano* **2011**, *5*, 1282−1290.

(15) Hizir, M. S.; Top, M.; Balcioglu, M.; Rana, M.; Robertson, N. M.; Shen, F. S.; Sheng, J.; Yigit, M. V. Multiplexed Activity of perAuxidase: DNA-Capped AuNPs Act as Adjustable Peroxidase. *Anal. Chem.* **2016**, *88*, 600−605.

(16) Zhang, L. N.; Deng, H. H.; Lin, F. L.; Xu, X. W.; Weng, S. H.; Liu, A. L.; Lin, X. H.; Xia, X. H.; Chen, W. In Situ Growth of Porous Platinum Nanoparticles on Graphene Oxide for Colorimetric Detection of Cancer Cells. *Anal. Chem.* **2014**, *86*, 2711−2718.

(17) Wu, G. W.; He, S. B.; Peng, H. P.; Deng, H. H.; Liu, A. L.; Lin, X. H.; Xia, X. H.; Chen, W. Citrate-Capped Platinum Nanoparticle as a Smart Probe for Ultrasensitive Mercury Sensing. *Anal. Chem.* **2014**, *86*, 10955−10960.

(18) Diez-Castellnou, M.; Mancin, F.; Scrimin, P. Efficient Phosphodiester Cleaving Nanozymes Resulting from Multivalency and Local Medium Polarity Control. *J. Am. Chem. Soc.* **2014**, *136*, 1158−1161.

(19) Zhang, W.; Hu, S.; Yin, J.-J.; He, W.; Lu, W.; Ma, M.; Gu, N.; Zhang, Y. Prussian Blue Nanoparticles as Multienzyme Mimetics and Reactive Oxygen Species Scavengers. *J. Am. Chem. Soc.* **2016**, *138*, 5860−5865.

(20) Liu, B. W.; Sun, Z. Y.; Huang, P. J. J.; Liu, J. W. Hydrogen Peroxide Displacing DNA from Nanoceria: Mechanism and Detection of Glucose in Serum. *J. Am. Chem. Soc.* **2015**, *137*, 1290−1295.

(21) Shen, X.; Liu, W.; Gao, X.; Lu, Z.; Wu, X.; Gao, X. Mechanisms of Oxidase and Superoxide Dismutation-like Activities of Gold, Silver, Platinum, and Palladium, and Their Alloys: A General Way to the Activation of Molecular Oxygen. *J. Am. Chem. Soc.* **2015**, *137*, 15882−15891.

(22) Cai, R.; Yang, D.; Peng, S.; Chen, X.; Huang, Y.; Liu, Y.; Hou, W.; Yang, S.; Liu, Z.; Tan, W. Single Nanoparticle to 3D Supercage: Framing for an Artificial Enzyme System. *J. Am. Chem. Soc.* **2015**, *137*, 13957−13963.

(23) Song, Y. J.; Xia, X. F.; Wu, X. F.; Wang, P.; Qin, L. D. Integration of Platinum Nanoparticles with a Volumetric Bar-Chart Chip for Biomarker Assays. *Angew. Chem., Int. Ed.* **2014**, *53*, 12451−12455.

(24) Lin, Y. H.; Ren, J. S.; Qu, X. G. Catalytically Active Nanomaterials: A Promising Candidate for Artificial Enzymes. *Acc. Chem. Res.* **2014**, *47*, 1097−1105.

(25) Wei, H.; Wang, E. Fe3O4 magnetic nanoparticles as peroxidase mimetics and their applications in H2O2 and glucose detection. *Anal. Chem.* **2008**, *80*, 2250−2254.

(26) Luo, W. J.; Zhu, C. F.; Su, S.; Li, D.; He, Y.; Huang, Q.; Fan, C. H. Self-Catalyzed, Self-Limiting Growth of Glucose Oxidase-Mimicking Gold Nanoparticles. *ACS Nano* **2010**, *4*, 7451−7458.

(27) Zheng, X. X.; Liu, Q.; Jing, C.; Li, Y.; Li, D.; Luo, W. J.; Wen, Y. Q.; He, Y.; Huang, Q.; Long, Y. T.; Fan, C. H. Catalytic Gold Nanoparticles for Nanoplasmonic Detection of DNA Hybridization. *Angew. Chem., Int. Ed.* **2011**, *50*, 11994−11998.

(28) Zhang, Y.; Wang, Z. Y.; Li, X. J.; Wang, L.; Yin, M.; Wang, L. H.; Chen, N.; Fan, C. H.; Song, H. Y. Dietary Iron Oxide Nanoparticles Delay Aging and Ameliorate Neurodegeneration in Drosophila. *Adv. Mater.* **2016**, *28*, 1387−1393.

(29) Liang, H.; Liu, B. W.; Yuan, Q. P.; Liu, J. W. Magnetic Iron Oxide Nanoparticle Seeded Growth of Nucleotide Coordinated Polymers. *ACS Appl. Mater. Interfaces* **2016**, *8*, 15615−15622.

(30) Zhao, H.; Dong, Y. M.; Jiang, P. P.; Wang, G. L.; Zhang, J. J. Highly Dispersed CeO2 on TiO2 Nanotube: A Synergistic Nanocomposite with Superior Peroxidase-Like Activity. *ACS Appl. Mater. Interfaces* **2015**, *7*, 6451−6461.

(31) Zhang, Z.; Hao, J. H.; Yang, W. S.; Lu, B. P.; Ke, X.; Zhang, B. L.; Tang, J. L. Porous Co3O4 Nanorods-Reduced Graphene Oxide with Intrinsic Peroxidase-Like Activity and Catalysis in the

DOI: 10.1021/acssensors.6b00500
ACS Sens. 2016, 1, 1336−1343

Degradation of Methylene Blue. *ACS Appl. Mater. Interfaces* **2013**, *5*, 3809−3815.
(32) Dong, J. L.; Song, L. N.; Yin, J. J.; He, W. W.; Wu, Y. H.; Gu, N.; Zhang, Y. Co3O4 Nanoparticles with Multi-Enzyme Activities and Their Application in Immunohistochemical Assay. *ACS Appl. Mater. Interfaces* **2014**, *6*, 1959−1970.
(33) Hu, P.; Han, L.; Dong, S. J. A Facile One-Pot Method to Synthesize a Polypyrrole/Hemin Nanocomposite and Its Application in Biosensor, Dye Removal, and Photothermal Therapy. *ACS Appl. Mater. Interfaces* **2014**, *6*, 500−506.
(34) Yang, Z. J.; Cao, Y.; Li, J.; Lu, M. M.; Jiang, Z. K.; Hu, X. Y. Smart CuS Nanoparticles as Peroxidase Mimetics for the Design of Novel Label-Free Chemiluminescent Immunoassay. *ACS Appl. Mater. Interfaces* **2016**, *8*, 12031−12038.
(35) Biella, S.; Prati, L.; Rossi, M. Selective oxidation of D-glucose on gold catalyst. *J. Catal.* **2002**, *206*, 242−247.
(36) Asati, A.; Santra, S.; Kaittanis, C.; Nath, S.; Perez, J. M. Oxidase-Like Activity of Polymer-Coated Cerium Oxide Nanoparticles. *Angew. Chem., Int. Ed.* **2009**, *48*, 2308−2312.
(37) Asati, A.; Kaittanis, C.; Santra, S.; Perez, J. M. pH-Tunable Oxidase-Like Activity of Cerium Oxide Nanoparticles Achieving Sensitive Fluorigenic Detection of Cancer Biomarkers at Neutral pH. *Anal. Chem.* **2011**, *83*, 2547−2553.
(38) Tonga, G. Y.; Jeong, Y. D.; Duncan, B.; Mizuhara, T.; Mout, R.; Das, R.; Kim, S. T.; Yeh, Y. C.; Yan, B.; Hou, S.; Rotello, V. M. Supramolecular regulation of bioorthogonal catalysis in cells using nanoparticle-embedded transition metal catalysts. *Nat. Chem.* **2015**, *7*, 597−603.
(39) Cheng, H. J.; Zhang, L.; He, J.; Guo, W. J.; Zhou, Z. Y.; Zhang, X. J.; Nie, S.; Wei, H. Integrated Nanozymes with Nanoscale Proximity for in Vivo Neurochemical Monitoring in Living Brains. *Anal. Chem.* **2016**, *88*, 5489−5497.
(40) Rydstrom, J. Evidence for a proton-dependent regulation of mitochondrial nicotinamide-nucleotide transhydrogenase. *Eur. J. Biochem.* **1974**, *45*, 67−76.
(41) Singh, N.; D'Souza, A.; Cholleti, A.; Sastry, G. M.; Bose, K. Dual regulatory switch confers tighter control on HtrA2 proteolytic activity. *FEBS J.* **2014**, *281*, 2456−2470.
(42) Liu, B. W.; Liu, J. W. Accelerating peroxidase mimicking nanozymes using DNA. *Nanoscale* **2015**, *7*, 13831−13835.
(43) Li, Y. Y.; He, X.; Yin, J. J.; Ma, Y. H.; Zhang, P.; Li, J. Y.; Ding, Y. Y.; Zhang, J.; Zhao, Y. L.; Chai, Z. F.; Zhang, Z. Y. Acquired Superoxide-Scavenging Ability of Ceria Nanoparticles. *Angew. Chem., Int. Ed.* **2015**, *54*, 1832−1835.
(44) Xu, C.; Liu, Z.; Wu, L.; Ren, J. S.; Qu, X. G. Nucleoside Triphosphates as Promoters to Enhance Nanoceria Enzyme- like Activity and for Single- Nucleotide Polymorphism Typing. *Adv. Funct. Mater.* **2014**, *24*, 1624−1630.
(45) Muhammad, F.; Wang, A.; Qi, W.; Zhang, S.; Zhu, G. Intracellular Antioxidants Dissolve Man-Made Antioxidant Nanoparticles: Using Redox Vulnerability of Nanoceria to Develop a Responsive Drug Delivery System. *ACS Appl. Mater. Interfaces* **2014**, *6*, 19424−19433.
(46) Tarnuzzer, R. W.; Colon, J.; Patil, S.; Seal, S. Vacancy engineered ceria nanostructures for protection from radiation-induced cellular damage. *Nano Lett.* **2005**, *5*, 2573−2577.
(47) Kim, C. K.; Kim, T.; Choi, I. Y.; Soh, M.; Kim, D.; Kim, Y. J.; Jang, H.; Yang, H. S.; Kim, J. Y.; Park, H. K.; Park, S. P.; Park, S.; Yu, T.; Yoon, B. W.; Lee, S. H.; Hyeon, T. Ceria Nanoparticles that can Protect against Ischemic Stroke. *Angew. Chem., Int. Ed.* **2012**, *51*, 11039−11043.
(48) Hayat, A.; Andreescu, S. Nanoceria Particles As Catalytic Amplifiers for Alkaline Phosphatase Assays. *Anal. Chem.* **2013**, *85*, 10028−10032.
(49) Ni, P.; Wei, X.; Guo, J.; Ye, X.; Yang, S. On the origin of the oxidizing ability of ceria nanoparticles. *RSC Adv.* **2015**, *5*, 97512−97519.
(50) Kwon, H. J.; Cha, M.-Y.; Kim, D.; Kim, D. K.; Soh, M.; Shin, K.; Hyeon, T.; Mook-Jung, I. Mitochondria-Targeting Ceria Nanoparticles as Antioxidants for Alzheimer's Disease. *ACS Nano* **2016**, *10*, 2860−2870.
(51) Peng, Y. F.; Chen, X. J.; Yi, G. S.; Gao, Z. Q. Mechanism of the oxidation of organic dyes in the presence of nanoceria. *Chem. Commun.* **2011**, *47*, 2916−2918.
(52) Xu, C.; Qu, X. Cerium oxide nanoparticle: a remarkably versatile rare earth nanomaterial for biological applications. *NPG Asia Mater.* **2014**, *6*, e90.
(53) Karakoti, A.; Singh, S.; Dowding, J. M.; Seal, S.; Self, W. T. Redox-active radical scavenging nanomaterials. *Chem. Soc. Rev.* **2010**, *39*, 4422−4432.
(54) Xu, X. L.; Chen, D.; Yi, Z. G.; Jiang, M.; Wang, L.; Zhou, Z. W.; Fan, X. M.; Wang, Y.; Hui, D. Antimicrobial Mechanism Based on H_2O_2 Generation at Oxygen Vacancies in ZnO Crystals. *Langmuir* **2013**, *29*, 5573−5580.
(55) Lakshmi Prasanna, V.; Vijayaraghavan, R. Insight into the Mechanism of Antibacterial Activity of ZnO: Surface Defects Mediated Reactive Oxygen Species Even in the Dark. *Langmuir* **2015**, *31*, 9155−9162.
(56) Miao, Y.; He, N.; Zhu, J.-J. History and New Developments of Assays for Cholinesterase Activity and Inhibition. *Chem. Rev.* **2010**, *110*, 5216−5234.
(57) Inestrosa, N. C.; Alvarez, A.; Pérez, C. A.; Moreno, R. D.; Vicente, M.; Linker, C.; Casanueva, O. I.; Soto, C.; Garrido, J. Acetylcholinesterase Accelerates Assembly of Amyloid-β-Peptides into Alzheimer's Fibrils: Possible Role of the Peripheral Site of the Enzyme. *Neuron* **1996**, *16*, 881−891.
(58) Liao, D.; Chen, J.; Zhou, H.; Wang, Y.; Li, Y.; Yu, C. In Situ Formation of Metal Coordination Polymer: A Strategy for Fluorescence Turn-On Assay of Acetylcholinesterase Activity and Inhibitor Screening. *Anal. Chem.* **2013**, *85*, 2667−2672.
(59) Liang, M.; Fan, K.; Pan, Y.; Jiang, H.; Wang, F.; Yang, D.; Lu, D.; Feng, J.; Zhao, J.; Yang, L.; Yan, X. Fe3O4Magnetic Nanoparticle Peroxidase Mimetic-Based Colorimetric Assay for the Rapid Detection of Organophosphorus Pesticide and Nerve Agent. *Anal. Chem.* **2013**, *85*, 308−312.
(60) Pezzato, C.; Prins, L. J. Transient signal generation in a self-assembled nanosystem fueled by ATP. *Nat. Commun.* **2015**, *6*, 7790.
(61) Lin, Y.; Huang, Y.; Ren, J.; Qu, X. Incorporating ATP into biomimetic catalysts for realizing exceptional enzymatic performance over a broad temperature range. *NPG Asia Mater.* **2014**, *6*, e114.
(62) Vernekar, A. A.; Das, T.; Mugesh, G. Vacancy-Engineered Nanoceria: Enzyme Mimetic Hotspots for the Degradation of Nerve. *Angew. Chem., Int. Ed.* **2016**, *55*, 1412−1416.
(63) Pautler, R.; Kelly, E. Y.; Huang, P. J.; Cao, J.; Liu, B. W.; Liu, J. W. Attaching DNA to Nanoceria: Regulating Oxidase Activity and Fluorescence Quenching. *ACS Appl. Mater. Interfaces* **2013**, *5*, 6820−6825.
(64) Liu, B. W.; Huang, Z. C.; Liu, J. W. Boosting the oxidase mimicking activity of nanoceria by fluoride capping: rivaling protein enzymes and ultrasensitive F^- detection. *Nanoscale* **2016**, *8*, 13562−13567.

DOI: 10.1021/acssensors.6b00500
ACS Sens. 2016, 1, 1336−1343